

TIPP 2011 – Technology and Instrumentation for Particle Physics 2011

Optimum Design of Quenching Capacitor Integrated Silicon Photomultipliers for TOF-PET Application

Gyuseong Cho^{a,*}, Hyoungtaek Kim^a, Woo Suk Sul^b, Chaehun Lee^c, Bo-Sun Kang^d

^a*Radiation Detection And Medical Image Sensor Laboratory, Department of Nuclear and Quantum Engineering, KAIST, Daejeon 305-701, Republic of Korea*

^b*National Nanofab Center, Daejeon 305-806, Republic of Korea*

^c*Samsung Advanced Institute of Technology, Gyeonggi Do 446-712, Republic of Korea*

^d*Department of Radiological Science, College of Medical Science, Konyang University, Daejeon, 302-718, Republic of Korea*

Abstract

The prototype SiPM was designed and fabricated for MRI compatible PET using the customized CMOS process at National Nanofab Center in KAIST. The SiPM was designed to have a size of $3 \times 3 \text{ mm}^2$ composed of micro-cells of $65 \times 65 \mu\text{m}^2$ with a fill factor of 68 %. The size of a micro-cell was determined by optimization between the photon detection efficiency (PDE) and the dynamic range for the photons of 511 keV from LYSO crystal. In the micro-cell structure, a specially designed quenching capacitor (QC) is added parallel to quenching resistor using the Metal-Insulator-Metal (MIM) process. This QC integrated SiPMs (QC-SiPM) was devised to realize rapid response of output pulses and to enhance the timing resolution of SiPM. Coincidence timing resolution of PET detectors depends on the output pulse shapes which are the convolution of the intrinsic pulse shape of scintillation crystals and the single photon pulse shape at the micro-cell in a SiPM. A quenching capacitor parallel to a quenching resistor provides a fast current path at the beginning stage of avalanche process, than reduces rising time of single photon pulse shape. In this study the rise time of the QC-SiPM signal was analyzed to be 22.5 ns while that for the regular SiPM was 34.3 ns.

© 2012 Published by Elsevier B.V. Selection and/or peer review under responsibility of the organizing committee for TIPP 11. Open access under [CC BY-NC-ND license](http://creativecommons.org/licenses/by-nd/3.0/).

Keywords : SiPM, TOF-PET, Quenching capacitor, Timing resolution

1. Introduction

In recent years, solid state photo-sensors have been studied for the PET (Positron Emission Tomography) application. Among various silicon based photo-sensors, the silicon photomultiplier (SiPM)

* Email: gscho@kaist.ac.kr

is the best candidate for PET detectors with its high gain, low operation voltage, low cost, compactness, as well as non-sensitivity to magnetic field for PET-MRI (Magnetic Resonance Imaging) application. We have designed and fabricated the quenching capacitor (QC) integrated SiPMs (QC-SiPM) for Time-Of-Flight PET (TOF-PET) application using customized CMOS process at National Nanofab Center in KAIST. The SiPM was designed to have a size of $3 \times 3 \text{ mm}^2$ composed of micro-cells (Geiger mode APDs) of $65 \times 65 \mu\text{m}^2$ with a fill factor of 66% for each micro-cell. The p-type epitaxial wafer with the resistivity of 11 ohm-cm and the thickness of 4.5 μm for the epitaxial layer was used to form shallow n+/p well junctions. In a micro-cell structure, a specially designed quenching capacitor (C_q) was added in parallel to the quenching resistor (R_q) made with the Metal-Insulator-Metal (MIM) process.

There is a large amount of statistical noise inherent to PET image reconstruction from the uncertainty of the annihilation photons' position along the line of response (LOR) [1, 2]. To overcome the poor inherent spatial resolution of PET, TOF-PET has been suggested [2, 3]. The accuracy of time of flight information depends on the timing resolution of detectors. The total timing resolution of PET detectors is usually determined by the timing uncertainties of 3 components as follows:

$$\sigma_{total} = \sqrt{\sigma_c^2 + \sigma_d^2 + \sigma_r^2} \quad (1)$$

where σ_c , σ_d and σ_r are the timing uncertainty from the crystal, the detector and the readout electronics respectively.

Commercially available scintillation crystals such as GSO, LYSO, and LaBr₃ have the fast rising and decay time characteristics adequate for TOF-PET applications. Solid-state photo-sensors have been developed to replace the traditional PMTs (Photomultiplier tubes) which have the very fast timing characteristics. Among various semiconductor photo-sensors, SiPMs are considered to be the best choice for TOF-PET application because of their fast timing characteristics and a high gain at a low operating bias, which are almost equivalent to PMTs.

A typical PET detector output has the same rise times with respect to a different pulse height of absorbed 511 keV annihilation photons, and the leading edge method is commonly used in TOF-PET application as a time pick-up. This leading edge method causes a timing uncertainty due to different signal amplitudes [4]. In order to reduce this uncertainty and improve the timing resolution, the ratio of the amplitude to the rise time of the output pulse has to be increased. There are two factors to reduce the timing uncertainty in SiPM: (1) high PDE and (2) fast rise time. These factors are dealt with in the successive parts of this paper.

In this study, optimum design of a QC-SiPM is presented. The size of the micro-cell and the junction structure were optimized for 511 keV gamma-ray photons and the LYSO crystal of $3 \times 3 \times 20 \text{ mm}^3$. The characteristics such as the photon detection efficiency (PDE), the dynamic range, the energy resolution of SiPM can be expressed as functions of the size of a micro-cell. With these relationships the optimum size for photons from an LYSO crystal can be evaluated. A quenching capacitor in parallel to a quenching resistor provides a fast current path at the beginning stage of an avalanche process so it reduces the rising time of a single photon pulse shape.

2. Optimization of structure

2.1. Dynamic range and PDE

The dynamic range of SiPMs should be compromised with the PDE of SiPMs. The dynamic range of SiPM is limited by the number of total micro-cells, and the PDE is reduced when the size of micro-cell is decreased as the increasing total number of micro-cells when the size of SiPM is fixed. Therefore the optimum size of a micro-cell for PET detectors coupled with an LYSO crystal should be calculated in order to increase the energy resolution and the dynamic range at 511 keV at the same time.

In a SiPM, PDE can be represented as a product of three terms.

$$\text{PDE} = QE \times P_t \times FF \quad (2)$$

where, QE is the quantum efficiency of a SiPM as a function of the incident photon wavelength and P_t is the probability of avalanche triggering as a function of electric field distribution inside the device [5] and FF is a geometrical efficiency indicating the fraction of the active area which is called as a fill factor. In terms of the micro-cell design, the PDE can be presented as a function of micro-cell size because the active area is limited by dead layers like the metal line, the poly-silicon resistor and the guard rings etc. The quantum efficiency and the triggering probability were estimated by TCAD simulation. Around 13 % of PDE is assumed at the wavelength of 420 nm and at 1 V over voltage for the size of $65 \times 65 \mu\text{m}^2$ micro-cell.

The dynamic range of SiPM is governed by the Poisson distribution as follows.

$$N_{\text{fired}} = N_{\text{cells}} \cdot \left(1 - e^{-\frac{\text{PDE} \cdot N_{\text{photons}}}{N_{\text{cells}}}}\right) \quad (3)$$

where, N_{fired} is the number of fired micro-cells and N_{cells} is the number of total micro-cells and N_{photons} is the number of incident photons. In Eq. (3), the PDE as a function of micro-cell size affect to the number of total micro-cells as shown in Fig. 1. The fill factor of SiPM is increased as the size of micro-cell increases, but the number of total micro-cells is reduced so the dynamic range is limited.

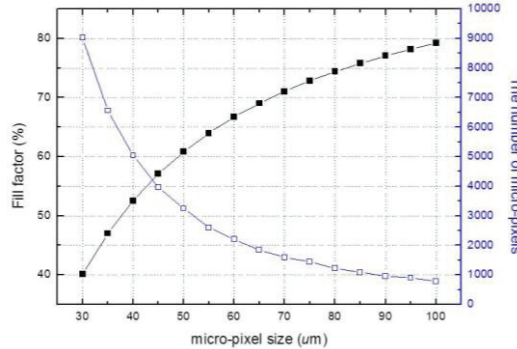


Fig.1. The fill factor and the number of micro-cells in a $3 \times 3 \text{ mm}^2$ SiPM

2.2. Energy resolution of SiPM

The energy resolution of SiPM is affected by both the PDE and the dynamic range of SiPM. The optimum size was considered in terms of the energy resolution. The energy resolution of SiPM can be expressed as follows [6]

$$R_{total} = \sqrt{R_0^2 + R_{statistic}^2} \quad (4)$$

$$R_0 = 2.35 \frac{1}{\sqrt{N_{cells}}} \frac{N_{cells}}{PDE \cdot N_{photons}} \sqrt{e^{\frac{N_{cells}}{PDE \cdot N_{photons}}} - 1 - \frac{PDE \cdot N_{photons}}{N_{cells}}} \quad (5)$$

$$R_{statistic} = 2.35 \frac{1}{\sqrt{N_{photons}}} \quad (6)$$

where, R_{total} is the total energy resolution and R_0 is the energy resolution of SiPM originated from non-linearity and $R_{statistic}$ is the energy resolution component due to the statistic distribution. The optimum size can be estimated with respect to the energy resolution as a function of a micro-cell size as shown in Fig. 2(a). The LYSO crystal has a high output of about 25,000 light photons/MeV and 40 ns decay time. The number of incident light from an LYSO crystal to the surface of SiPM within the recovery time is assumed to be about 3,000 photons [7, 8]. Using these values the micro cell size of $65 \times 65 \mu\text{m}^2$ was determined and the measured energy resolution of a prototype SiPM is around 15 % at 511 keV with a LYSO coupling in Fig. 2(b).

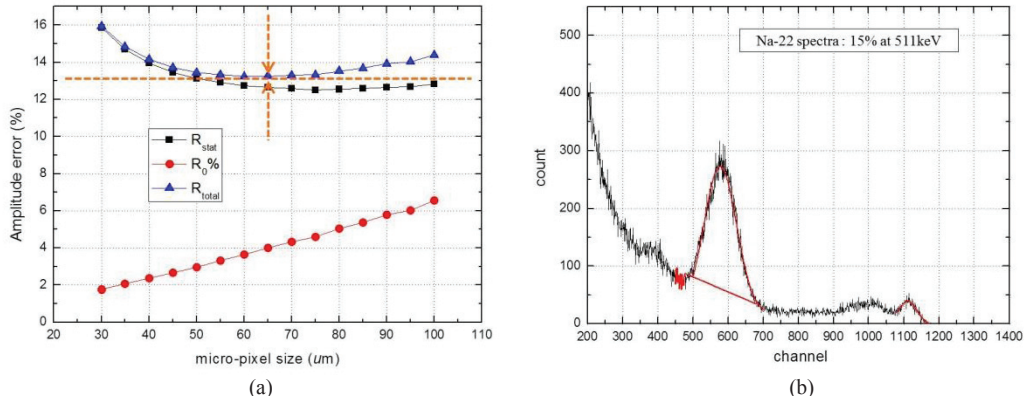


Fig.2. Calculated value of amplitude error with respect to the micro-cell size (a) and measured Na-22 energy spectra of SiPM which is designed as optimum cell size (b).

3. Quenching Capacitor Integrated SiPM

3.1. Pulse shape of normal SiPM

The SiPM is an array of several thousand of micro-cells which are operated in Geiger-mode independently. A micro-cell generally consists of a PN diode (C_d), a series resistance (R_d), a quenching resistor (R_q), and any parasitic capacitor (C_q) in parallel to the quenching resistor. When an avalanche breakdown happens, the amount of generated charge per an initial carrier is in the order of 10^6 . The current from a micro cell has two phases. First the current is extinguished by passing through a quenching

resistor during the quenching time (τ_q) which is $(R_q||R_d)(C_q+C_d)$. Second the diode is recharged to the applied bias during the recovery time (τ_r) which is $(C_q+C_d)R_d$ [9]. The pulse shape of a micro cell with a quenching capacitor can be modeled as follows [4].

$$I_{GAPD_rise}(t) = \frac{1}{R_q + R_d} \left(1 - e^{-\frac{t}{\tau_q}} \right) + \frac{C_q}{(C_q + C_d)R_d} e^{-t/\tau_q} \quad (7)$$

$$I_{GAPD_decay}(t) = \frac{C_d}{\tau_r} e^{-t/\tau_r} \quad (8)$$

where, $I_{GAPD_rise}(t)$ is the rising component of the avalanche current during the quenching phase and $I_{GAPD_decay}(t)$ is the decay component during the recharging phase. In Eq. (7), the avalanche current possesses a spike-like component of $C_q/((C_d+C_q)R_d)$ but this component is not seen because the quenching capacitor is usually small with the range of 1~3 femto-farad.

3.2. Effect of MIM quenching capacitor

To use SiPMs in TOF-PET, the timing resolution has to be improved further. The coincidence timing resolution of PET detectors depends on the output pulse shapes which are again the convolution of the intrinsic rise and decay times of scintillation crystals and the single photon pulse shape of a SiPM micro-cell. A large fraction of avalanche current in the decay component causes a poor timing performance. Therefore the timing performance can be improved by increasing the fraction of avalanche current in the rising component. There are several tries to modify the signal shape like by adding clipping capacitance in readout circuit to shorten the SiPM response [10]. In this study, a quenching capacitor (C_q) was added parallel to the quenching resistor (R_q) because C_q can provide a fast current path in the beginning of the avalanche process. The single photon pulse shape of a micro-cell and the output pulse shape of the QC-SiPM were modelled through SPICE circuit simulator [4]. The equivalent circuit of a QC-SiPM is shown in Fig. 3. The quenching capacitor of 30 fF was determined from the simulation results and was fabricated using Metal-Insulator-Metal (MIM) capacitor without any reduction of the fill factor.

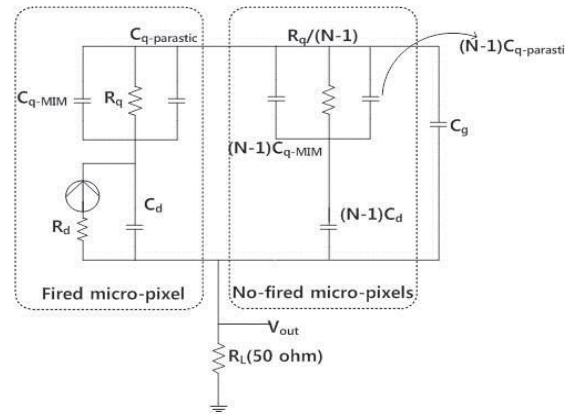


Fig.3. Equivalent circuit of a QC-SiPM

3.3. Pulse shape of C_q integrated SiPM

The single photon pulse shape of a SiPM was recorded by 2GHz oscilloscope. A single micro-cell was separately designed as a test pattern to analyze the single photon pulse shape of SiPM. 1ns pulsed LED light was sent to a micro-cell which was connected to a $50\ \Omega$ load resistor in order to exclude any other distortions from readout electronics. As shown in Fig. 4, the QC-SiPM has a sharper peak in the rising part than the regular SiPM. This means that the initial avalanche current is passed through the quenching capacitor. The recharging of the SiPM is not affected because the recharging current is very slow compared to the quenching current. The quenching capacitor plays a role in a low impedance path at high frequency region and a high impedance path at low frequency region. The measured data is well fitted to SPICE simulated curve. The gamma-ray signal with an LYSO crystal coupled was also measured and is given in Fig. 5. The measurement setup is almost the same as the single photon pulse measurement set-up except the light source is replaced by a gamma-ray source. The rise time of 22 ns was achieved in the QC-SiPM compare to 34 ns of the regular SiPM. The QC-SiPM has a faster rise time because the output signal of the QC-SiPM is the convolution of light emission from LYSO which has most photons in the initial part and the faster single photon pulse shape.

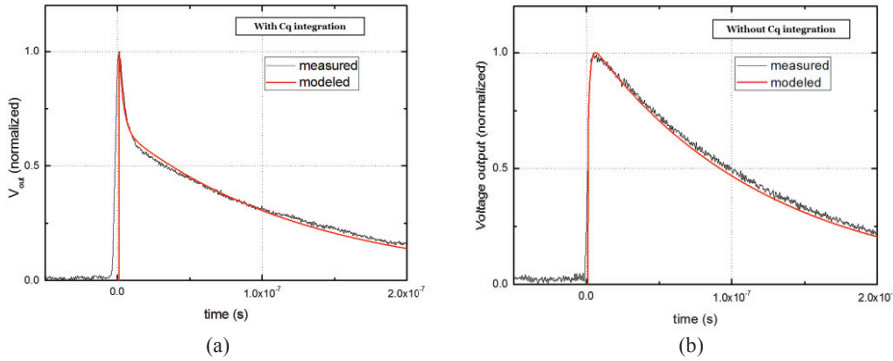


Fig.4. Single-photon pulse shape of SiPM with (a), and without quenching resistor (b). Both measured photon pulses are normalized for comparison.

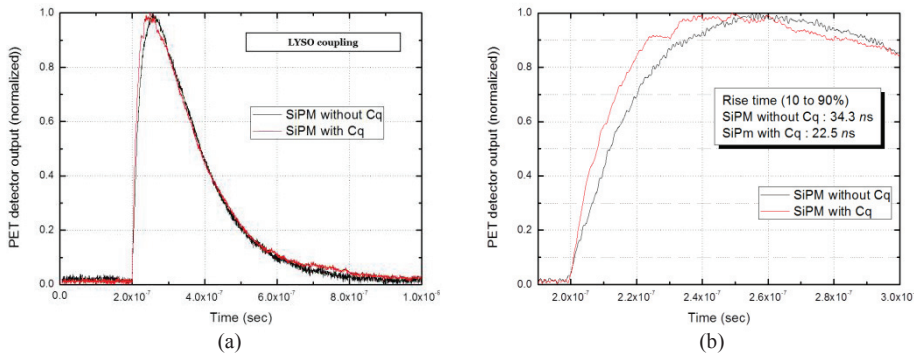


Fig.5. Output pulse shape of SiPM with LYSO crystal coupling. The whole signal (a) and the rising part (b)

4. Conclusion

The image quality of PET systems can be improved with TOF information which confines the LOR with respect to the timing resolution, consequently TOF increases the SNR in the PET image by reducing the statistical background noise. The timing resolution of PET detectors should be improved in order to obtain TOF information. The timing resolution is directly related to the amplitude to the rise time ratio of PET detectors. As the ratio increases, the timing performance can be enhanced. In this study the pulse shape of the proposed QC-SiPM of $3 \times 3 \text{ mm}^2$ was studied to embody the TOF-PET detector with coupling to an LYSO crystal. A dedicated SiPM for PET, especially for TOF-PET, was designed and fabricated in the customized CMOS process at National Nanofab Center. A key performance parameter, the PDE of SiPM, was carefully modeled with consideration of the fill factor and the dynamic range in order to optimize the energy resolution of the SiPM at the 511 keV gamma-ray energy after coupling with an LYSO of $3 \times 3 \times 20 \text{ mm}^3$. A QC-SiPM was designed and fabricated using an MIM quenching capacitor, C_q , to enhance the timing resolution. The rise time of a PET detector with the QC-SiPM was 22.5 ns while the regular SiPM has 34.3 ns.

Acknowledgements

This study was supported by the R&D Program of MKE/KEIT [10030104, Development of Silicon Photomultiplier, and PET-MRI fusion system].

References

- [1] William W. Moses, Nucl. Instr. and Meth. A 580 (2007) 919.
- [2] T. Back, et al., Nucl. Instr. and Meth. A 477 (2002) 82.
- [3] Nizar A. Mullani, et al., J. Nucl. Med. 21 (1980) 1095.
- [4] C. Lee, et al., Nucl. Instr. and Meth. A 650 (2011) 125-128.
- [5] R. J. McIntyre, IEEE Trans. Electron Devices, vol. ED-20, no. 7 (1973) 637-641.
- [6] A. Stoykov, et al., J. Instr. vol. 2, 2007, p. P06005
- [7] M. Mazzillo, et al., IEEE Trans. Nucl. Sci., vol. 56, no 4, pp. 2434-2442, Aug. 2009.
- [8] C. L. Melcher, et al., IEEE Trans. Nucl. Sci., vol. 39, no 4, pp. 502-505, 1992.
- [9] Gin-Chung Wang, IEEE Trans. Nucl. Sci. NS57 (2010) 25.
- [10] A. Ronzhin, et al., Nucl. Instr. and Meth. A 668 (2012) 94-97.